# Supplementary Data

## Supplementary Materials

### *Bacterial strains and plasmids*

*Streptomyces reticuli* and *Streptomyces lividans* (*S. reticuli* and *S. lividans*, respectively) as well as the *Escherichia coli* strains BL21(DE3)pLysS and DH5α were used. The plasmid constructs pETHbpS (38) were taken to introduce specific mutations into the *hbpS* gene (see below). The plasmid construct pUKS10 (35) was used to generate the *S. reticuli cpeB* disruption mutant.

### *Generation of* S. reticuli *cpeB disruption mutant*

The blunt-ended *Sgf*I-*Srf*I fragment of the plasmid pUKS10 was ligated with the *Sma*I-cutted pUC18 vector, thus leading to the plasmid construct pUFC. The blunt-ended *Pst*I-*Pst*I fragment—containing the kanamycin-resistance gene *ahp*I—of the plasmid pUCK4 (Amersham Biosciences) was ligated with the larger and blunt-ended *Stu*I-*Eco*N1 fragment of pUFC. The resulting plasmid pUFKC contained *ahp*I that is flanked on the left by 0.55 kb (representing the 5′-end of *cpeB*) and on the right by 0.5 kb (representing the 3′-end of *cpeB*) of pUFC. To modify the ends of restricted DNAs, the Klenow enzyme (Fermentas) was used. Ten micrograms of the isolated pUFKC construct were denaturated (0.2 M NaOH, 10 min, 37°C), chilled on ice, and neutralized by rapid addition of HCl. Then, the DNA was used to transform 50 μl of protoplasts ($\sim 10^9$/ml) generated from *S. reticuli* that were spread onto osmotically stabilized medium and incubated at 30°C for 19 h. The plates were overlaid with 2 ml of molten agarose (40°C) containing kanamycin (500 μg/ml). Kanamycin-resistant colonies were restreaked several times, and then, their genomic DNA was analyzed as to the size of fragments carrying the kanamycin gene.

As the wild-type strain, the obtained *S. reticli cpeB* mutant does not have any growth defect during cultivation in minimal medium.

### *Growth assays*

The sensitivity of *S. reticuli* wild-type (WT) and *S. reticuli cpeB* mutant against the redox stressors $H_2O_2$, cumene hydroperoxide, and plumbagin was determined by using a disk inhibition assay. A sample of 100 μl spores ($5 \times 10^8$) was added to 3 ml soft agar poured onto the respective R2 plates (23) and allowed to solidify. Sterile 6 mm-diameter blank papers disks (Schleicher & Schuell) were added to the bacteria-overlaid plates and saturated with 20 μl of $H_2O_2$ (0.25% or 0.5%), cumene hydroperoxide (0.25% or 0.5%), or plumbagin (100 mM), respectively. Plates were incubated overnight at 30°C before zones of inhibitions were measured.

### *Viability tests*

Spores ($0.5 \times 10^5$) of *S. reticuli* strains were inoculated in minimal medium (MM) containing 1% galactose and cultivated overnight at 30°C. Subsequently, plumbagin (20 μM) was added in to the culture, and cultivation was prolonged for 1 h. Cultures were subjected to a viability assay by using the DEAD/LIFE®-BacLight Kit™ (Invitrogen) and the microscope Axio Observer Z1 (Zeiss). Examinations were done under UV by using filter sets (Zeiss) for FITC (excitation, HQ 480/40; beam splitter, Q 505 LP; emission, HQ 535/50) and Texas red (HQ 560/55, Q 595 LP, HQ 645/75, respectively). This assay involves differential staining of damaged (dead) cells with propidium iodide, which can only enter damaged (dead) cells and subsequently intercalate into the DNA, thus leading to red fluorescence. Living hyphae can take up the dye SYTO 9 that interacts with DNA, thus leading to green fluorescence (32).

### *Polyacrylamide gel electrophoresis and Western blotting*

Proteins were separated by 10% or 12% polyacrylamide gel electrophoresis (PAGE) in the presence or absence of sodium dodecyl sulfate (SDS). Subsequently, gels were stained with Coomassie blue or transferred to a fluorotrans membrane and treated with anti-HbpS or anti-CpeB antibody

### *Site directed mutagenesis*

Point mutations in the *hbpS* gene on the plasmid pETHbpS were introduced by PCR. To obtain HbpSGly71Cys, the following primers (5′→3′) were used: PG71Cfor (GCG***CC ATGG***CCGACAC-CACGGAGG) and PG71Crev (GCT***CGTA CG***ACTGCGGGCCCGC**GCA**GTCCCCGCGCAGGG). The restriction sites for *Nco*I (in PG71C) or *Bsi*WI (in PG71Crev) are written in bold and italics. The codon encoding cysteine (in PG71C) is underlined and written in bold. The numbering of the amino acids is in agreement with the sequence of the 3D structure of HbpS (protein data bank [PDB]: 3FPV). After PCR, the amplicon was restricted with *Nco*I and *Bsi*WI, and ligated with the larger *Nco*I-*Bsi*WI fragment of pETHbpS. The ligation products were entered into *E. coli* DH5α. Subsequently, the obtained plasmid construct was analyzed with restriction enzymes and by sequencing. The resulting correct plasmid was named pETHbpSGly71Cys. To generate HbpSSer139Cys-Gly71Cys, the shorter *Nco*I-*Bsi*WI fragment of pETHbpSGly71Cys was ligated with the larger *Nco*I-*Bsi*WI fragment of pETSer139Cys (26). Ligation products were entered into *E. coli* DH5α. Finally, the correctness of the ligation was proved by sequencing. To overproduce the corresponding proteins, the plasmids pETHbpSGly71Cys and pETHbpSSer139Cys-Gly71Cys were used to transform *E. coli* BL21 (DE3) pLysS.

### *Production, purification, and analyses of HbpS proteins*

Protein production and purification were performed as described earlier (38), using Ni-NTA affinity chromatography, TEV protease cleavage, and anion exchange chromatography over a DEAE-sepharose column. The purity of the His-tag free HbpS protein solutions (WT, Ser139Cys, Gly71-Cys, and Ser139Cys-Gly71Cys) was controlled by SDS-PAGE and by mass spectrometry analysis (ESI LC-MS). The

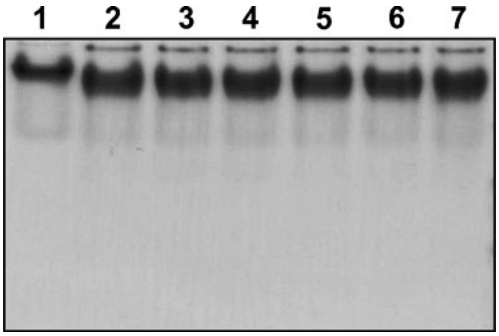


**SUPPLEMENTARY FIG. S1. Oligomeric assembly of HbpS proteins**. Wild-type (lane 1), Ser139Cys (lane 2), Ser139R (lane 3), Gly71Cys (lane 4), Gly71R (lane 5), Ser139-Cys-Gly71Cys (lane 6), and Ser139R-Gly71R (lane 7) HbpS proteins were separated by native PAGE and stained with Coomassie. The apparently slightly faster migration of the mutants can be attributed to the presence of the hydrophobic amino acid cysteine that in each case has replaced a hydrophilic amino acid (serine or glycine). Moreover, the additional protein form with apparently higher molecular weight might represent proteins forming intermolecular disulfide bridges.

concentration of purified HbpS proteins was calculated from their absorbance at 280 nm, assuming an $\varepsilon_{280}$ of 8250 $M^{-1}$ $cm^{-1}$ (molecular mass = 15,498 Da). Secondary structures of isolated proteins were analyzed by circular dichroism spectroscopy as previously described (26). In parallel, native PAGE experiments were performed to determine their assembly state under standard conditions (25).

### *Continuous wave electron paramagnetic resonance measurements*

Room temperature continuous wave electron paramagnetic resonance (cw EPR) spectra were recorded on a Miniscope X-band benchtop EPR spectrometer (MS200; Magnetech GmbH) equipped with a rectangular TE102 resonator. The microwave power was set to 10 mW and the B-field modulation to 0.125 mT. 20 $\mu$l of sample volume containing 100 $\mu$M protein were filled in EPR glass capillaries (0.9 mm inner diameter).

Cw EPR spectra for inter-spin distance determination in the range from $\sim$ 0.8 to 2.0 nm were obtained on a homemade cw X-band EPR spectrometer equipped with a Super High Sensitivity Probehead (Bruker Biospin GmbH). The magnetic field was measured with a B-NM 12 B-field meter (Bruker Biospin GmbH). A continuous flow cryostat Oxford ESR900 (Oxford Instruments) was used in combination with an Intelligent Temperature Controller (ITC 4; Oxford Instruments), thus allowing the stabilization of the sample temperature to 160 K. The microwave power was set to 0.2 mW and the B-field modulation amplitude to 0.25 mT. EPR quartz capillaries (3 mm inner diameter) were filled with sample volumes of 40 $\mu$l. Fitting of simulated dipolar broadened EPR powder spectra to the experimental ones detected at 160 K was carried out by using the program DipFit (33).

### *Pulse EPR measurements*

Pulse EPR (DEER) experiments were carried out at X-band frequencies (9.3–9.5 GHz) with a Bruker Elexsys 580 spectrometer equipped with a Bruker Flexline split-ring resonator

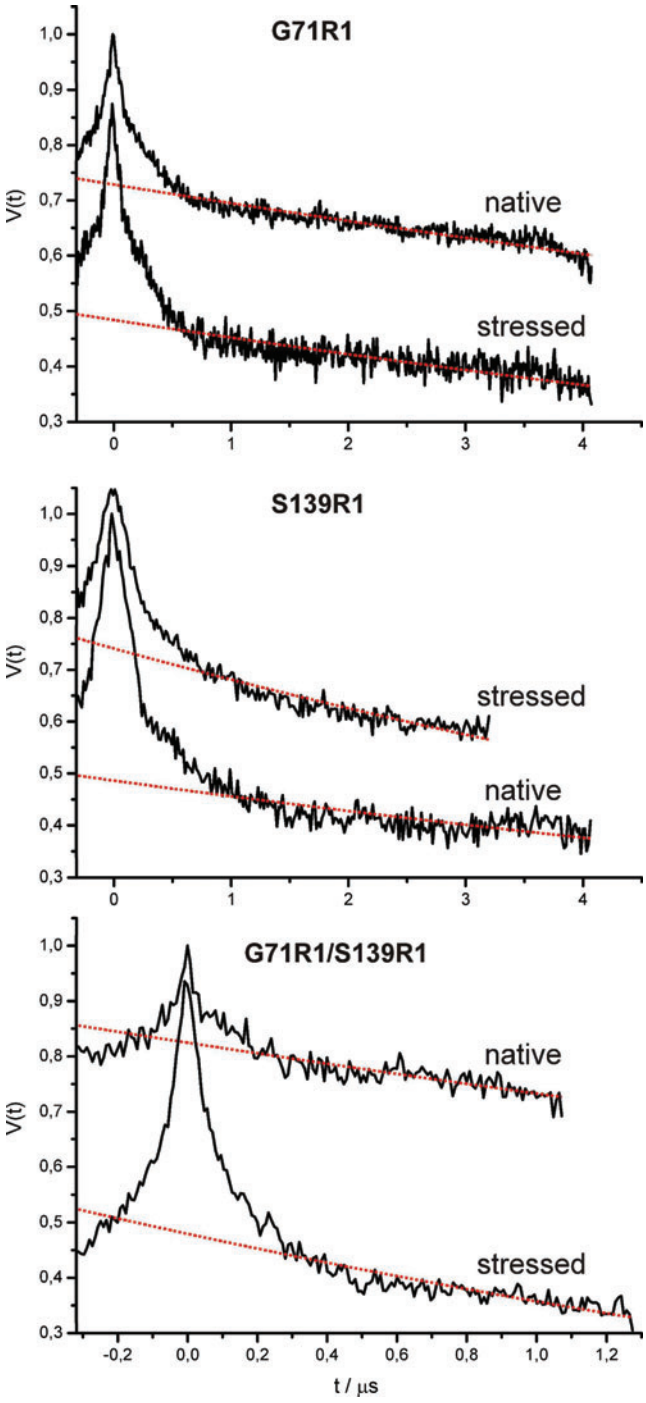


**SUPPLEMENTARY FIG. S2. Dipolar evolution data (raw DEER traces, V(t)) for HbpS-Gly71R1 (*top*), HbpS-Ser139R1 (*middle*), and the double mutant Gly71R1/Ser139R1 (*bottom*).** In all cases, the DEER traces for the unstressed (native) and the stressed samples are shown and accordingly labeled. Red dotted line represents the background functions used for correction, yielding the background corrected dipolar evolution functions (Form Factors, F(t)) shown in Figure 4 in the main text.

ER 4118X-MS3 and a continuous flow helium cryostat (ESR900; Oxford Instruments) controlled by an Oxford Intelligent Temperature Controller ITC 503S. Spin diluted samples have been prepared by mixing the spin-labeled protein with the corresponding unlabeled HbpS in a 1:4 molar ratio.

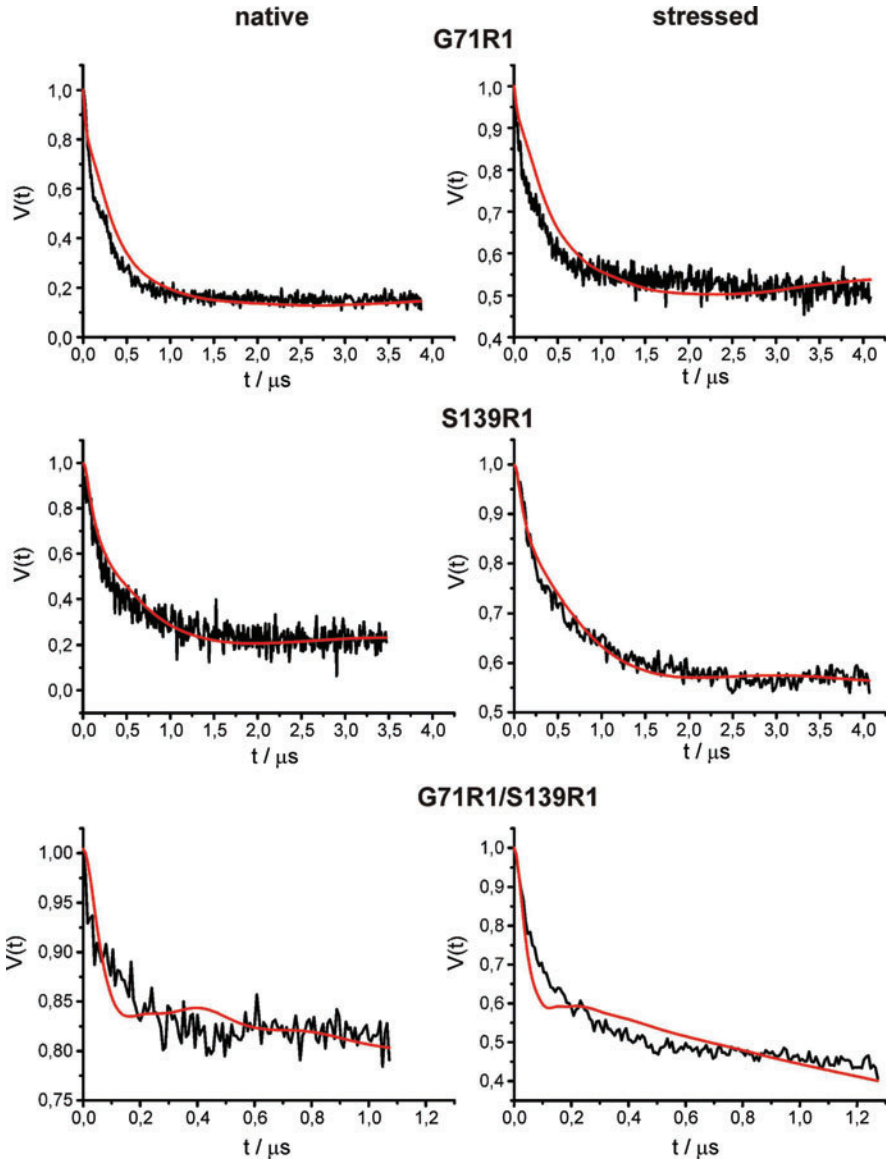


**SUPPLEMENTARY FIG. S3. Comparison of the (zero time corrected) dipolar evolution data with the predicted primary data from the RLA.** *Left*: native HbpS mutant, *right*: stressed HbpS mutants. Experimental DEER data have been loaded into MMM after execution of the respective RLA. The modulation depths were fitted to allow a direct comparison of the accordance of the simulated with the experimental primary data. The comparison between the experimental and the simulated primary data reveals reasonable fits for HbpS-Ser139R1 in native and stressed form, significant differences for Gly71R1 also in both states especially in the 0–1 $\mu$s region (corresponding to the short distance range), and clear deviations for the double mutant Gly71R1/Ser139R1, thus underlining that the experimental distance distribution for the double mutant differs significantly from the RLA prediction.

All measurements were performed by using the four-pulse DEER sequence: $\pi/2$ ($\nu_{obs}$) - $\tau_1 - \pi$ ($\nu_{obs}$) $- t' - \pi$ ($\nu_{pump}$) $-$ ($\tau_1 + \tau_2 - t'$) $- \pi$ ($\nu_{obs}$) $- \tau_2 -$ echo (16, 28). A two-step phase cycling ($+\langle x\rangle$, $-\langle x\rangle$) was performed on $\pi/2$ ($\nu_{obs}$). Time $t'$ is varied, whereas $\tau_1$ and $\tau_2$ are kept constant, and the dipolar evolution time is given by $t = t' - \tau_1$. Data were analyzed only for $t > 0$. The resonator was overcoupled to Q $\sim$ 0–100; the pump frequency $\nu_{pump}$ was set to the center of the resonator dip and coincided with the maximum of the nitroxide EPR spectrum, whereas the observer frequency $\nu_{obs}$ was 65–67 MHz higher, coinciding with the low field local maximum of the spectrum. All measurements were performed at a temperature of 50 K with observer pulse lengths of 16 ns for $\pi/2$ and 32 ns for $\pi$ pulses and a pump pulse length of 12 ns. Deuterium modulation was averaged by adding traces at eight different $\tau_1$ values, starting at $\tau_{1,0} =$ 400 ns and incrementing by $\Delta\tau_1 =$ 56 ns. $D_2O$ buffer with deuterated glycerol was used in all cases for their effect on the phase relaxation. Data points were collected in 8 ns time steps or, if the absence of fractions in the distance distribution below an appropriate threshold was experimentally checked, in 16 ns time steps. The total measurement time for each sample was 8–32 h. Analysis of the data was performed with DeerAnalysis 2010 (10).

*Rotamer library analysis*

In the rotamer library approach (RLA), the canonical ensemble of possible spin label side chain conformations is modeled by a discrete set of 210 precalculated rotamers (29). From the RLA, a conformational distribution of R1 at any chosen position in the otherwise fixed protein structure can be determined as described in detail in (29). Briefly, the superposition of R1's backbone atoms onto the protein backbone at the respective position provides the orientation of R1 with regard to the protein structure and allows to calculate a resulting energy for the R1-protein interaction from the Lennard Jones potential by using the MD force field CHARMM27 (15). Subsequent Boltzmann weighting and normalization by the partition function yields a probability for each rotamer that is then multiplied by the probability of R1 to exhibit each conformation. This results in the final rotamer probability distribution at the site of interest. Between two such probability distributions at two positions in the protein, a distance distribution is calculated as the histogram of all pairwise interspin distances weighted by the product of their respective probabilities. The rotamer library analyses in this study have been carried out by using the modeling program MMM Version 2010 (29) (www.epr.ethz.ch/software/index), in which the RLA is implemented, on the crystal structures of HbpS (protein data bank [PDB]: 3FPV for native HbpS in the octameric state; 3FPW for the HbpS-iron complex, monomer).

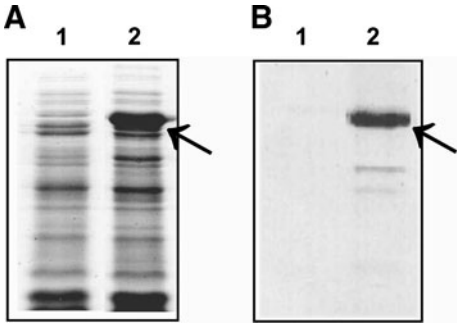


**SUPPLEMENTARY FIG. S4. Mycelia-associated proteins were released from *Streptomyces lividans* pWHM3 (lane 1; lacking *cpeB*) and *S. lividans* pWKS13 (lane 2; harboring *cpeB*) using 0.01% Triton X-100 (see Material and Methods in main text).** These proteins were subjected to 10% sodium dodecyl sulfate–polyacrylamide gel electrophoresis, and either stained with Coomassie **(A)** or transferred to a fluorotrans membrane for Western analysis by using anti-CpeB antibodies **(B)**. The *arrow* indicates the position of CpeB.